Journal of Robotics and Control (JRC)
Volume 5, Issue 1, 2024
ISSN: 2715-5072, DOI: 10.18196/jrc.v5i1.20519

Adaptive Cruise Control of the Autonomous Vehicle Based on Sliding Mode Controller Using Arduino and Ultrasonic Sensor

Rachid Alika [1*], El Mehdi Mellouli [2], El Houssaine Tissir [3]
[1, 3] Department of Physics, LISAC Laboratory, Faculty of Sciences Dhar El Mehraz, Sidi Mohamed Ben Abdellah University, Fez, Morocco
[2] National School of Applied Sciences, LISA Laboratory, Sidi Mohamed Ben Abdellah University, Fez, Morocco
Email: [1] rachid.alika@usmba.ac.ma, [2] mellouli_elmehdi@hotmail.com, [3] elhoussaine.tissir@usmba.ac.ma
*Corresponding Author

***Abstract*—This article will focus on adaptive cruise control in autonomous automobiles. The adaptive cruise control inputs are the safety distance which determines thanks to conditions set depending on the distance value, the measured distance, the longitudinal speed of the autonomous automobile itself, the output is the desired acceleration. The objective is to follow the vehicles in front with safety, according to the distance measured by the ultrasonic sensor, and maintain a distance between the vehicles in front greater than the safety distance which we have determined. For this, we used super twisting sliding mode controller (STSMC) and non-singular terminal sliding mode controller (NTSMC) based on neural network applied to the adaptive cruise control system. The neural network is able to approximate the exponential reaching law term parameter of the NTSMC controller to compensate for uncertainties and perturbations. An autonomous automobile adaptive cruise control system prototype was produced and tested using an ultrasonic sensor to measure the distance between the two automobiles, and an Arduino board as a microcontroller to implement our program, and four DCs motors as actuators to move or stop our host vehicle. This system is processed by code and Simulink Matlab, the efficiency and robustness of these controllers are excellent, as demonstrated by the low longitudinal velocity error value. The safety of autonomous vehicles can be enhanced by improving adaptive cruise control using STSMC and NTSMC based on neural network controllers, which are chosen for their efficiency and robustness.**

Keywords—Autonomous Vehicle; Adaptive Cruise Control; Sliding Mode Controller; Ultrasonic Sensor; Non-Singular Terminal Sliding Mode Controller; Neural Network; Autonomous Vehicle Safety; Efficiency Improvement; Robustness Improvement.

I. INTRODUCTION

Autonomous vehicles equipped with an ACC (Adaptive Cruise Control) system represent a major advancement in automotive technology. Autonomous vehicles [1]-[6] are vehicles capable of moving without human intervention, thanks to a combination of sensors and software [7]-[9]. They are now the center of interest for researchers. The study of lateral dynamics is found in [10][11], and vertical dynamics in [12][13]. ACC is an advanced speed control system that allows vehicles to automatically maintain a safe distance from vehicles in front while adjusting their speed based on real-time traffic [14][15]. Autonomous vehicles equipped with ACC have the advantage of reducing road accidents, improving traffic flow, and reducing fuel consumption.

Our aim is to create a prototype of an autonomous vehicle that is equipped with ACC and can track lead vehicles in complete safety. The components, such as the Arduino Uno as the microcontroller [16]-[21], the DC motor as the driving force [7][16], and the Ultrasonic HC-SR04 as the sensor [16], are essential elements to build this prototype.

The process of operating an Arduino board-based adaptive cruise control (ACC) involves several steps, beginning with vehicle host detection and ending with speed regulation. Firstly, use the ultrasonic sensor to measure the distance between lead vehicle and the host vehicle, and then transmit the distance data to the Arduino board. The Arduino board analyzes the sensor data to detect the distance between the host vehicle and the vehicle in front, based on the current distance and preset parameters, the ACC controller calculates the desired speed to maintain a safe distance from the vehicle in front. Then the Arduino board sends commands to the DC motor actuators, which allow the host vehicle to drive at the calculated desired speed.

The controller used in this study is the sliding mode controller (SMC) [22]-[26] with the following two types, super twisting sliding mode controller (STSMC) and non-singular terminal sliding mode controller (NTSMC), these types of controllers have the advantage of avoiding uncertainties and disturbances. They are included in the nonlinear controller and applied to multi-input, multi-output (MIMO) systems, and have led to good performances, but in this work, we need to implement them in hardware to observe more.

The focus of this research will be both on theoretical design, simulation and hardware implementation. We added an ACC program as a Matlab function in a Simulink blocks in order to implement this ACC program in a microcontroller. For a simple implementation, the Arduino microcontroller would be used. Low cost, small size and wide applications [16] are all advantages of using Arduino. The use of Arduino encourages practical learning. Students

can quickly move from theory to practice by creating real-world projects such as sensors, robots, and other interactive devices, strengthening their understanding of fundamental concepts. Students receive immediate feedback while experimenting with Arduino. They can see the results of their code in real time, making it easier to understand errors and fix problems. This helps to develop the skills needed to tackle technical challenges in the real world. Therefore, it will be advantageous for the educational purpose and the implementation of the material.

The integration of artificial intelligence techniques [27]-[30] is necessary for the development of the studied system. The use of neural networks [31]-[33] to approximate functions or terms has several benefits, which include modeling complex non-linear functions and adapting parameters. The effectiveness of neural networks in approximating terms depends on the quality and quantity of the training data, as well as the appropriate choice of network architecture. The neural network [23] is being exploited to improve our non-singular sliding mode controller. A study of lateral dynamics of autonomous vehicles by sliding mode control based on fuzzy logic [34]. Sliding mode control based on particle swarm optimization (PSO) is used to control the lateral dynamics of autonomous vehicles [35][36].

Our work focused on the study of adaptive cruise control of autonomous vehicles in a theoretical and practical way. The STSMC and neural network-based NTSMC controllers are used in this study. The study is divided into two parts. In the first part, we carried out a theoretical study on the adaptive cruise control of the host vehicle with the aim of keeping a safe distance from the lead vehicle. The comparison of our proposed controller with the RBF_NTSMC controller used in [37] and with HMP [38] has been carried out and the results obtained by our proposed method are better. We created a prototype of an autonomous vehicle that was equipped with adaptive cruise control (ACC) in the second part and subjected it to various tests. These tests are carried out according to three possible safety distance situations, the host automobile exists at a distance greater than the maximum safety distance, then at a distance less than the maximum safety distance, and finally at a critical safety distance. The illustrations demonstrate the robustness of the controllers developped in the theoretical part. And in the practical part, our autonomous automobile prototype passed the various tests with success.

A. Related Works

In [39], the authors proposed a composite longitudinal controller for speed regulation of unmanned vehicles. A composite longitudinal control strategy integrating a steady-state controller and an active disturbance rejection state feedback controller is designed for speed regulation control during acceleration and deceleration.

In [40], the authors have studied a T-S fuzzy model predictive control framework is applied to the problem of adaptive cruise control (ACC). Variations in the preceding vehicle velocity and road surface conditions are considered to formulate adaptive cruise control as a tracking control problem of a T-S fuzzy system subject to parameter uncertainties and external persistent perturbations.

In [41], the authors realized a parking distance controller based on Arduino Uno using ultrasonic sensors. Three main components, namely Arduino UNO, Arduino MP3 Shield and ultrasonic HC-SR04. The prototype method steps are the design, writing of the system, implementation of the parking prototype and testing of its validity.

An ultrasonic sensor was utilized by the authors to create a fully automated cruise control system [42]. A microcontroller and ultrasonic obstacle detector have been used to develop an automatic vehicle speed control system.

In ref. [43], the authors developed an adaptive cruise control based on fuzzy logic using a remote control car, controlled by an Arduino Uno R3 board and used an ultrasonic sensor mounted on the front of the car.

B. Motivation

The research is motivated by the desire to contribute to the development of robust and adaptive control systems. STSMC and NTSMC_NN (neural networks) are used to improve stability and control performance, particularly in terms of efficiency and robustness.

The creation of an autonomous automobile prototype based on the study of an adaptive cruise control (ACC) is motivated by several factors which aim to improve the safety and efficiency of autonomous driving, and also to provide a solid basis for further development of this technology. ACC is a fundamental part of the autonomous driving system. By creating a prototype based on this technology, the project contributes to the development and deeper understanding of the technologies needed to make vehicles fully autonomous. The validation of this prototype and the identification of the challenges to develop it through the integration of new technologies is our essential motivation.

C. Novelties and Contributions of this Paper are as Follows:

- We propose a neural network-based NTSMC controller with a choice of reaching law expression and a neural network structure able of controlling the longitudinal dynamics of autonomous vehicles by improving the performance of ACC. Neural networks allow for the estimation of the reaching law term parameter. This is an innovative approach that can enhance control performance, particularly in terms of its effectiveness and robustness.
- Our proposal was to create a prototype of an autonomous automobile that focused on the study of ACC. This study has several advantages, including the validation of a prototype, and this prototype could serve as a practical demonstration of the ACC system, which is a key part of the autonomous driving system. This contributes to the advancement of technology in this area.

The document will be organized as follows. The introduction takes up the first section of the document. The

second section is the design of autonomous vehicles and controllers. Then, the next section is the hardware configuration in which we have defined the essential components and we have given the functional diagram of this prototype. The following section includes the results and discussion related to numerical simulation and hardware implementation. The final section is devoted to conclusions and future work.

II. SYSTEM MODELING DESIGN

A. Vehicle Dynamics Longitudinal Model

The study of the longitudinal dynamics of autonomous vehicles uses Newton's second law motion as follows,

$$\sum F = ma \tag{1}$$

In Equation (1), the symbol $\sum F$ signifies the summation of all forces exerted upon the vehicle. Within this equation, m represents the combined mass of the vehicle, while a denotes the vehicle's acceleration. The summation of all forces $\sum F$, can be detailed as follows.

$$\sum F = F_x - F_w - F_r - F_g \tag{2}$$

the force denoted as F_x represents the driving force generated by the vehicle's engine. F_w accounts for the aerodynamic drag. F_r represents the rolling resistance. Lastly, F_g represents the vehicle's gravitational force.

The model wheel dynamics is given by this equation,

$$I_w\dot{\omega} = -F_x R_\omega + T_p - T_b \tag{3}$$

where $T_p = T_e/r_g$ [44].

From equation (3), the force F_x is given as follows,

$$\mathrm{F}_x = \frac{1}{R_\omega}(T_e/r_g - T_b - I_w\dot{\omega})$$

The aerodynamic drag is written as follows,

$$F_w = \frac{1}{2}C_D A\rho {v_x}^2$$

The rolling resistance is given as follow,

$$F_r = mgfcos(\theta)$$

The gravity resistance of the vehicle is given by,

$$F_g = mgsin(\theta)$$

where T_p is the propulsion (drive) torque, T_e is the engine torque, r_g is gear ratio, T_b is Brake torque, I_w the inertia of wheel car, ω is the angular velocity, R_ω is the rolling radius, C_D is coefficient of the aerodynamic drag, A is the area of the front surface of the vehicle, ρ is the air density, v_x is the longitudinal velocity, m is the vehicle mass, g is the acceleration caused by gravity, f is the coefficient of rolling resistance and θ represents the road's angle of inclination.

From equations (1) and (2) we can write,

$$m\ddot{x} = F_x - F_w - F_r - F_g \tag{4}$$

We replace the existing forces in equation (2), we obtain,

$$m\dot{v_x} = \frac{1}{R_\omega r_g}T_e - \frac{1}{R_\omega}T_b - \frac{I_w}{{R_\omega}^2}\dot{v_x} - \frac{1}{2}C_D A\rho {v_x}^2 - mgfcos(\theta) - mgsin(\theta)$$

Finally, the longitudinal acceleration can be written as follows,

$$\dot{v_x} = \frac{R_\omega}{(m{R_\omega}^2 + I_w)r_g}T_e - \frac{R_\omega}{(m{R_\omega}^2 + I_w)}T_b - \frac{{R_\omega}^2}{(m{R_\omega}^2 + I_w)}[\frac{1}{2}C_D A\rho {v_x}^2 + mgfcos(\theta) + mgsin(\theta)] \tag{5}$$

We can represent the equation in the following manner,

$$\ddot{x} = f(x,t) + g(x,t)u \tag{6}$$

with $f(x,t) = -\frac{R_\omega}{(m{R_\omega}^2+I_w)}T_b - \frac{{R_\omega}^2}{(m{R_\omega}^2+I_w)}\left[\frac{1}{2}C_D A\rho {v_x}^2 + mgfcos(\theta) + mgsin(\theta)\right]$, $g(x,t) = \frac{R_\omega}{(m{R_\omega}^2+I_w)r_g}$ are the continuous functions and $u = T_e$ is the input control.

B. Profile Speed

The velocity tracking which we considered as reference velocity is illustrated in Fig. 1,

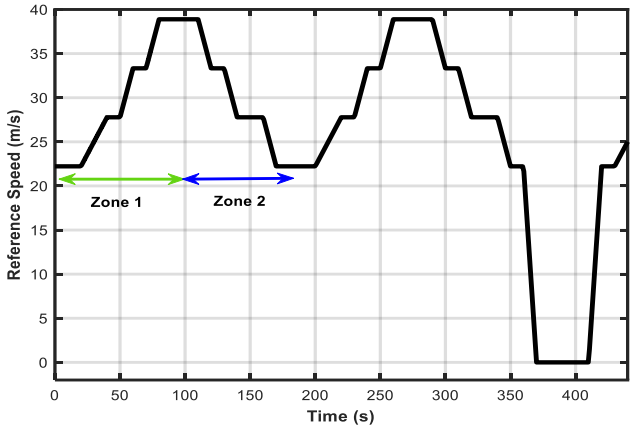

Fig. 1. Reference longitudinal speed

C. Control Strategy

The controller is made up of two parts, the upper controller and the lower controller. In this part of our study, we conduct a theoretical study on adaptive cruise control, also known as an upper controller, which uses an algorithm to determine the minimum and maximum distance safety conditions, see Fig. 4. And a theoretical analysis of a lower controller that attains adequate longitudinal speed to ensure the host vehicle follows the lead vehicle, see Fig. 2.

The study on the lower controller was carried out using the super twisting sliding mode controller (STSMC) and non-singular terminal sliding mode controller (NTSMC) based on neural networks. The controllers work in such a way that the controlled vehicle must maintain a safe distance and follow the lead vehicle safely. The NN-NTSMC method with the adaptation of the parameters of the neural network to the controller by the Lyapunov method was carried out.

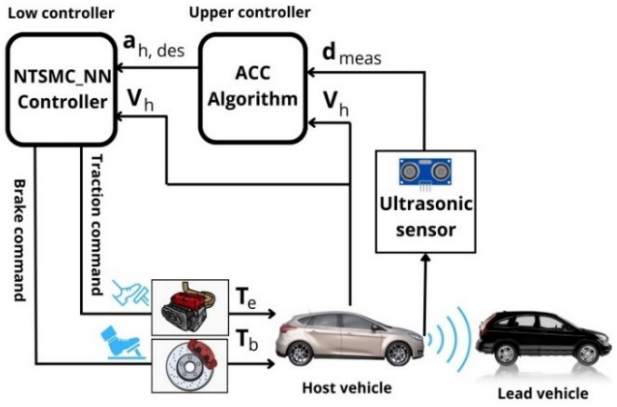

Fig. 2. Block diagram of the control strategy

1) *Design of Adaptive Cruise Controller*

The upper controller, called adaptive cruise control, is a longitudinal speed regulator which allows the longitudinal speed to be adjusted according to the distance between the two automobiles. This safety distance determined by certain conditions of maximum and minimum distance value, according to the following ACC Algorithm which we have implemented. If the measured distance is greater than the maximum safety distance, the vehicle is accelerated according to a desired speed (Zone 1), If the measured distance is between the minimum and maximum safety distance, the vehicle is decelerated according to a desired speed (Zone 2) see Fig. 1, and if the measured distance is less than or equal to a minimum safety distance, the vehicle is stopped. The output of this controller is the desired longitudinal acceleration and the inputs are the measured distance, the longitudinal speed of the host vehicle see Fig. 3.

The output of the upper controller is the desired longitudinal acceleration [14][45], which is the input to the lower controller from which either a traction command or a braking command is generated to control the host vehicle, see Fig. 2.

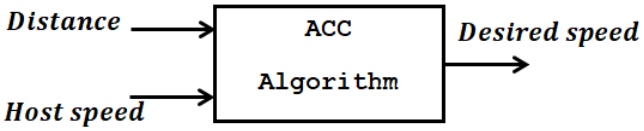

Fig. 3. Upper controller of the ACC

The ACC controller functions are accomplished according to the next algorithm:

Algorithm: ACC

Input: d_{meas}, v_h
Output: $a_{h,\ des}$
if $d_{meas} > d_{safe,\ max}$

Vehicle accelerates according to a reference speed of zone 1 profile.

elseif $d_{meas} <= d_{safe,\ max}$ ***and*** $d_{meas} > d_{safe,\ min}$

Vehicle decelerates according to a reference speed of zone 2 profile.

elseif $d_{meas} <= d_{safe,\ min}$

Vehicle stopping.

end

The ACC algorithm is represented in Fig. 4 by a flowchart.

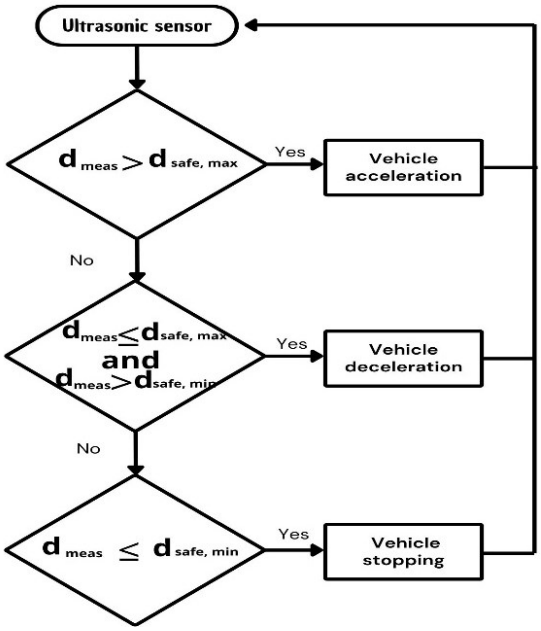

Fig. 4. Flowchart of ACC algorithm

2) *Radial Basis Function Neural Network*

The radial basis function neural network (RBFNN) is a multilayered neural network. It employs six layers. The RBFNN has a single output layer and the Gaussian function is the activation function in hidden layers [46][47]. The structure of RBFNN is shown as Fig. 5.

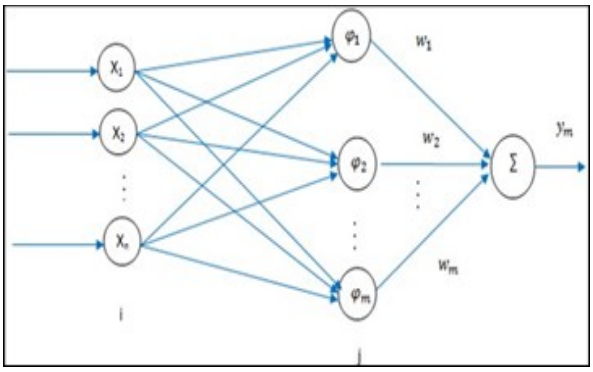

Fig. 5. RBFNN structure

The vector of RBF is $\varphi = [\varphi_j]^T, j = 1, \dots, m$, φ_j in the j^{th} hidden layer is the value of Gaussian function, $x = [x_i]^T$, $i = 1, \dots, n$, is an input vector.

$$\varphi_j(x_i) = \exp\left(-\frac{\sum_{i=1}^{n}|x_i - c_{ij}|^2}{2b_j^{\ 2}}\right)$$

where the Gaussian function has the parameters,

$$\boldsymbol{c} = [\mathbf{c_{ij}}] = \begin{bmatrix} \mathbf{c_{11}} \cdots \mathbf{c_{1m}} \\ \cdot \cdots \cdot \\ \cdot \cdots \cdot \\ \cdot \cdots \cdot \\ \mathbf{c_{n1}} \cdots \mathbf{c_{nm}} \end{bmatrix}$$ is the coordinate value of centre point of neural network j for the i^{th} input. b_j is the width value of Gaussian function for neural network j.

The radial basis function has a weight value:

$$W = [\mathrm{W}_1, \dots, \mathrm{W}_\mathrm{m}]^\mathrm{T}$$

The output of RBF is as follows:

$$y_m(t) = W^T\varphi = W_1\varphi_1 + W_2\varphi_2 + \cdots + W_m\varphi_m$$

3) Design of Neural Network Based Adaptive Non-Singular Terminal Sliding Mode Controller

The non-singular terminal sliding mode controller is composed of two parts, the equivalent control part $\mathrm{u_{EQ}}$ and another complementary part called the exponential reaching law $\mathrm{u_{ER}}$,

$$u = u_{EQ} + u_{ER}$$

with $u_{ER} = -ksign(s) - \mu s, k > 0, \mu > 0.$

To apply the non-singular terminal sliding mode controller to the vehicle's longitudinal dynamics, two essential steps are included. The initial step involves defining the nonsingular sliding surface, which is done as,

$$s = \int e_x dt + \frac{1}{\rho} {e_x}^{p/q} \tag{7}$$

where $\rho > 0$, p, q $(p > q)$ are positive odd numbers and e_x denotes the difference between the actual speed v_x and the targeted longitudinal speed v_{ref}, which can be expressed as,

$$e_x = v_x - v_{ref} \tag{8}$$

We have the time derivative of (7) that is,

$$\dot{s} = e_x + \frac{1}{\rho}(p/q){e_x}^{(p/q)-1}\dot{e_x} = e_x + \frac{1}{\rho}(p/q){e_x}^{(p/q)-1}(\dot{v}_x - \dot{v}_{ref}) \tag{9}$$

We replace equation (6) in equation (9), we obtain,

$$\dot{s} = e_x + \frac{1}{\rho}(p/q){e_x}^{(p/q)-1}(f(t,x) + g(t,x)u(t) - \dot{v}_{ref})$$

The second step consists in determining the longitudinal control.

$$u = u_{EQ} + u_{ER}$$

For the system dynamics to be optimal, the control law is,

$$\begin{aligned} u^*(x,w) &= u_{EQ} + {u^*}_{ER}(x,w) \\ {u^*}_{ER}(x,w) &= -k^*(x,w)sign(s) - \mu s, k^* > 0 \end{aligned} \tag{10}$$

where w is weight value of neural network.

Our approach involves the development of a neural network system with the objective of approximating a key parameter within the exponential reaching law. We obtain the equivalent control when $\dot{s} = 0$,

$$u_{EQ}(t) = -\frac{1}{g(t,x)}[\rho(q/p){e_x}^{(2-p/q)} + f(t,x) - \dot{v}_{ref}] \tag{11}$$

with $1 < p/q < 2$.

We present the adaptive neural network controller,

$$u(x,w) = u_{EQ} + \hat{u}_{ER}$$

where $\hat{u}_{ER}(x,w) = -\hat{k}(x,w)sign(s) - \mu s$ with $\hat{k}(x,w) = \hat{w}^T\varphi(x)$ is the parameter estimated by neural network. And $\hat{w}$ is the vector of the estimated weights value of neural network, and $\varphi(x)$ is the vector of radial basis function.

Following the neural network's approximation of the control law, denoted as $\hat{u}_{ER}(x,w)$ in reference [48], we can express Equation (6) as follows,

$$\ddot{x} = f(t,x) + g(t,x)(u_{EQ}(t) + \hat{u}_{ER}) \tag{12}$$

We have

$$\tilde{u}_{ER}(x,w) = \hat{u}_{ER}(x,w) - {u^*}_{ER}(x,w) \tag{13}$$

With

$$\tilde{u}_{ER}(x,w) = -\tilde{k}(x,w)sign(s) - \mu s \tag{14}$$

From equation (13), the equation (12) becomes,

$$\begin{aligned} \ddot{x} = f(t,x) + g(t,x)\big(&u_{EQ}(t) + {u^*}_{ER}(x,w) \\ &+ \tilde{u}_{ER}(x,w)\big) \end{aligned} \tag{15}$$

Replace (10), (11) and (14) in (15),

$$\begin{aligned} \ddot{x} = f(t,x) + g(t,x)\Big(&-\frac{1}{g(t,x)}\big[\rho(q/p){e_x}^{(2-p/q)} \\ &+ f(t,x) - \dot{v}_{ref}\big] - k^*sign(s) \\ &- \mu s - \tilde{k}(x,w)sign(s) - \mu s\Big) \end{aligned} \tag{16}$$

$$\begin{aligned} \ddot{x} = \dot{v}_{ref} - \rho(q/p){e_x}^{(2-p/q)} \\ + g(t,x)(-k^*(x,w)sign(s) \\ - \tilde{k}(x,w)sign(s) - 2\mu s) \end{aligned}$$

Replace (16) in (9),

$$\begin{aligned} \dot{s} = -\frac{1}{\rho}(p/q){e_x}^{(p/q)-1}g(t,x)((k^* + \tilde{k})sign(s) \\ + 2\mu s \end{aligned} \tag{17}$$

We can define the exponential reaching law by,

$$\hat{u}_{ER}(x,w) = -\hat{k}(x,w)sign(s) - \mu s$$

with $\hat{k}(x,w) = \hat{w}^T\varphi(x)$, and $\tilde{w} = \hat{w} - w^*$

The term ${u^*}_{ER}(x,w)$ can be expressed as,

$${u^*}_{ER}(x,w) = {u^*}_{ER}(x,w^*) + \epsilon$$

ϵ represents the approximation error associated with the neural network system, and $\epsilon \le |\epsilon|_{max}$. Consequently $k^*(x,w) = k^*(x,w^*) + \epsilon$.

From (13), $\tilde{\mathrm{k}}(\mathrm{x},\mathrm{w}) = \hat{\mathrm{k}}(\mathrm{x},\mathrm{w}) - \mathrm{k}^*(\mathrm{x},\mathrm{w})$, therefore $\tilde{\mathrm{k}}(\mathrm{x},\mathrm{w})$ becomes,

$$\begin{aligned} \tilde{k}(x,w) &= \hat{w}^T\varphi(x) - (w^{*T}\varphi(x) + \epsilon) \\ \tilde{k}(x,w) &= \tilde{w}^T\varphi(x) - \epsilon \end{aligned} \tag{18}$$

Replace (18) in (17),

$$\begin{aligned} \dot{s} = -\frac{1}{\rho}(p/q){e_x}^{(p/q)-1}g(t,x)(k^* + \tilde{w}^T\varphi(x) \\ - \epsilon)sign(s) \\ - \frac{1}{\rho}(p/q){e_x}^{(p/q)-1}g(t,x)(2\mu s) \end{aligned}$$

The Lyapunov function can be defined as follows,

$$V = \frac{1}{2}\, s^2 + \frac{1}{2\gamma}\, \tilde{w}\tilde{w}^T$$

The derivative of the Lyapunov function V is,

$$\dot{V} = s\dot{s} + 1/\gamma\ (\dot{\tilde{w}})\tilde{w}\hat{}T$$

$$= s(-\frac{1}{\rho}(p/q)e_x{}^{(p/q)-1}g(t,x)(\tilde{w}^T\varphi(x) - \epsilon + k^*)sign(s)$$

$$-\ \frac{1}{\rho}(p/q)e_x{}^{(p/q)-1}g(t,x)(2\mu s)) + \frac{1}{\gamma}\ \dot{\tilde{w}}\tilde{w}^T$$

$$\dot{V} = \tilde{w}^T\ (\frac{1}{\gamma}\ \dot{\tilde{w}} - \frac{1}{\rho}(p/q)e_x{}^{(p/q)-1}g(t,x)\ s\varphi(x)sign(s)) - s\frac{1}{\rho}(p/q)e_x{}^{(p/q)-1}g(t,x)(k^* - \epsilon)sign(s) - \frac{1}{\rho}(p/q)e_x{}^{(p/q)-1}g(t,x)(2\mu s^2)$$

If we let, $\eta = 2\mu$ and the adaptive law is,

$$\dot{\hat{w}} = \ \gamma s\ \frac{1}{\rho}(p/q)e_x{}^{(p/q)-1}g(t,x)\ \varphi(x)sign(s)$$

therefore, $\dot{V} = -\frac{1}{\rho}(p/q)e_x{}^{(p/q)-1}g(t,x)\ [(k^* - \epsilon)|s| + \eta s^2]$. Choosing $\eta > -(k^* - |\epsilon|_{max})\frac{|s|}{s^2} + \eta_0, \eta_0 > 0$, then,

$$\dot{V} \le -\eta_0 \frac{1}{\rho}(p/q)e_x{}^{(p/q)-1}g(t,x)s^2 < 0$$

To uphold the stability of the autonomous vehicle, certain conditions must be met.

Firstly, the value $\dot{\hat{w}}$ should adhere to the equation $\dot{\hat{w}} = \gamma\ \frac{1}{\rho}(p/q)e_x{}^{(p/q)-1}g(t,x)\varphi(x)|s|$. Additionally, the value of η must satisfy the inequality $\eta > -(k^* - |\epsilon|_{max})\frac{|s|}{s^2} + \eta_0$, where $\eta = 2\mu$, and $g(t,x)$ is required to be positive.

III. HARDWARE SIMULATION

A. Hardware Design

The system shown in Fig. 6 includes an ultrasonic sensor, four DC motors, an L298N motor driver [49], a battery, an LCD 1602 display [50], and a switch. The connections between these components play a crucial role in the proper functioning of the whole [16][51][52].

The Arduino is responsible for coordinating the operations of all the components, acting as the brain. The ultrasonic sensor is connected to the Arduino to measure the distance. The Arduino program utilizes the sensor output signal to determine decisions based on the measured distance. The four DC motors are connected to the L298N driver, which acts as an H-bridge to control the direction and speed of the motors. The battery powers the L298N driver, ensuring sufficient power to the motors. The LCD 1602 is connected to the Arduino to display crucial information in real time, providing a user interface. The switch is integrated to facilitate easy management of system power.

1) Arduino Uno Microcontroller

The Arduino Uno [53-55] is a popular and widely used microcontroller board for building electronic projects, especially in the field of embedded systems and robotics. There are 20 I/O pins on the Arduino Uno, 6 of them analog and 14 of them digital, of which 6 can be used for PWM (Pulse width Modulation) outputs.

2) Ultrasonic Sensor

The ultrasonic sensor [56-58] works by sending sound waves from the transmitter on which it is fixed, these waves bounce off an object (lead vehicle) and then return to the receiver (host vehicle). The distance of the object can be calculated by measuring the time it takes for sound waves to travel to the object and return to the sensor.

$$Distance\ =\ (Time * Speed\ of\ Sound)/2$$

3) Motor DC Actuator

DC motors [59]-[61] are continuous actuators that generate mechanical energy from electrical energy. Continuous angular rotation is generated by the DC motor, which can be utilized to rotate wheels, pumps, and fans. The DC motor, or Direct Current motor, is the most commonly used actuator to produce continuous motion and whose rotational speed can be easily controlled, making it ideal for use in applications such as control speed, and position control. To control the speed of the DC motor, it's simply a matter of controlling its input voltage.

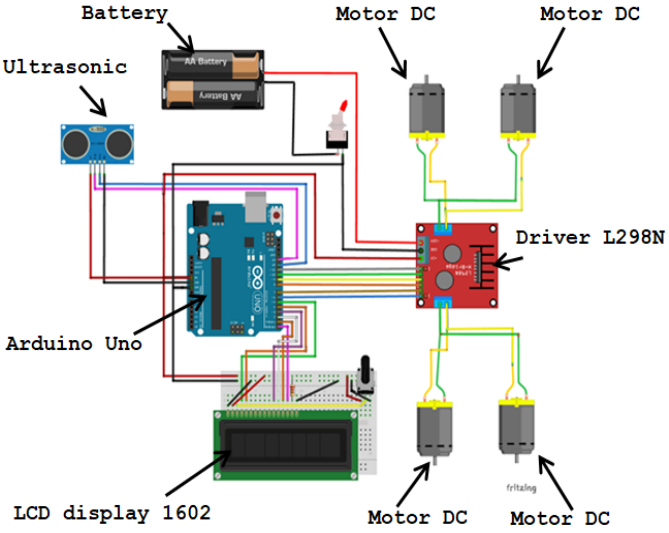

Fig. 6. The overall series of hardware configurations: arduino microcontroller circuit with ultrasonic

The autonomous vehicle shown in Fig. 7 is composed of three essential elements, an Ultrasonic sensor to detect the distance of the vehicle in front, the Arduino Uno board is used to implement our ACC program which controls the distance between automobiles, and the four DC Motor actuators are responsible for moving the automobile autonomously.

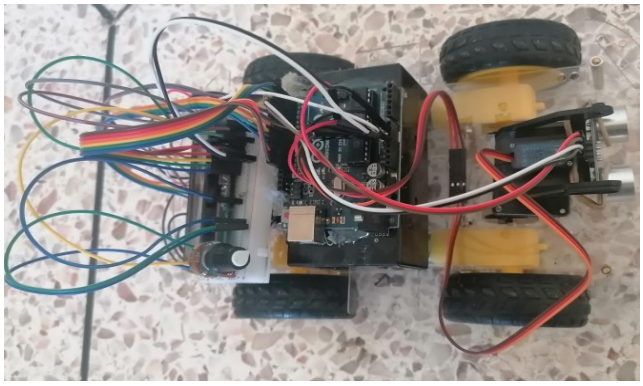

Fig. 7. Autonomous vehicle prototype

Our experience in Fig. 8 consists of two autonomous automobiles, the automobile which exists in front controlled by Bluetooth remote, and the host automobile on which we mounted the ACC controller.

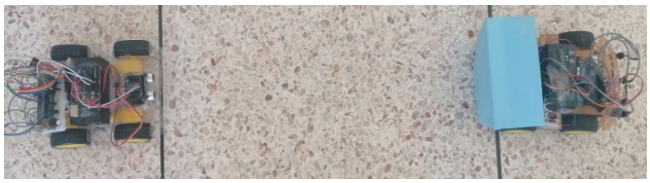

Fig. 8. Lead and host vehicles

IV. Results and Discussion

In this section, we have combined the functions of Matlab and Simulink Matlab presented in Fig. 9, in order to implement our ACC program in the autonomous vehicle prototype mentioned in Fig. 7.

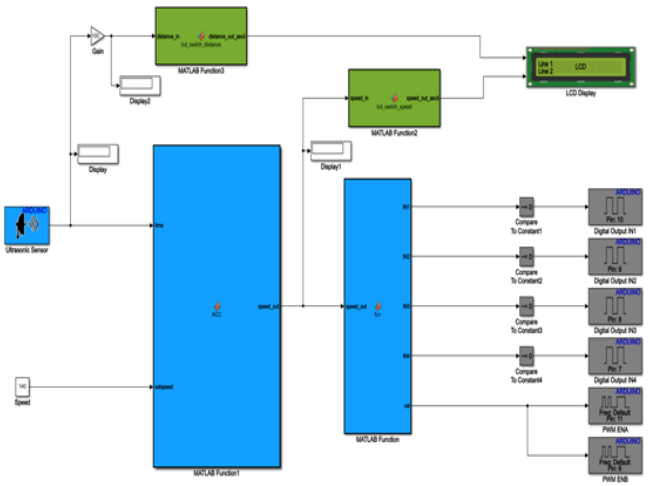

Fig. 9. Adaptive cruise control simulink model

A scenario has been provided to test the operation of our autonomous vehicle prototype, different distance values between the two automobiles are chosen to test different possible situations. These distance values are presented in Table I.

Table I presents the functioning principle of the host vehicle control and the obtained practical results. Our prototype passes all the tests that we submitted to it, see Table I.

TABLE I. Ultrasonic Sensor Testing

Distance	*Procedure*	*Expected results*	*Validation*
d_{meas}>100 cm	If the host vehicle is farther from the lead vehicle by a distance greater than 100 cm.	The longitudinal speed of the host vehicle is increased.	Success: Speed increase of host vehicle is performed
50 cm< d_{meas} and d_{meas}≤100 cm	If the distance between the host vehicle and the lead vehicle is greater than equal to 50 cm and less than or equal to 100 cm.	The longitudinal speed of the host vehicle is decreased.	Success: Speed decrease of host vehicle is performed
d_{meas}≤50 cm	If the host vehicle is further from the lead vehicle by a distance less than or equal to 50 cm.	The autonomous automobile prototype is stopped	Success: The vehicle is stopped

To test our prototype and validate our theoretical design control law, we have applied the profile distance shown in Fig. 10 and described in the following:

- In the first case where the distance is greater than 100 cm.
- In the second case, the distance is less than 100 cm and greater than 50 cm.
- In the third case, the distance is greater than 100 cm and the speed of our controlled automobile was greater than 0, which means that the automobile is not stopped.
- In the fourth case, the distance is less than 50 cm.
- In the fifth case, the distance is greater than 100 cm and our automobile was stopped due to a distance limitation (distance less than 50 cm).

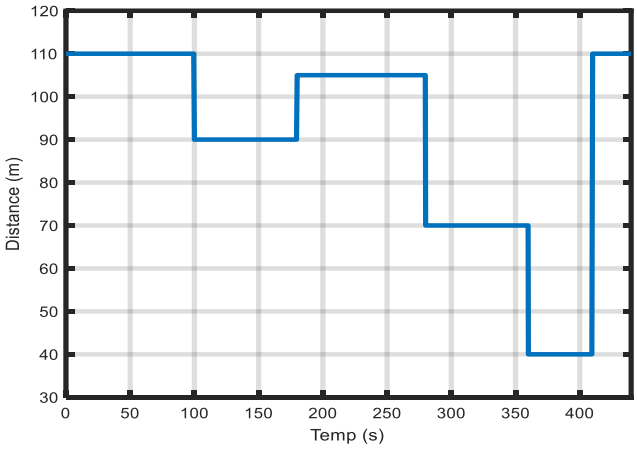

Fig. 10. Profile distance

Our autonomous automobile prototype has successfully passed all tests, see video in https://shorturl.at/jkP08. The video content introduces two vehicles, the lead vehicle is controlled by Bluetooth to move forward and stop this automobile in order to test the ACC operations, and the host vehicle is our prototype which is equipped with an ultrasonic sensor, an Arduino Uno board and Wheels powered by a DC motor actuator. In this video, the lead vehicle is placed at a distance greater than 100 cm, and the

host vehicle starts first and it is seen that it moves forward with an increase in speed, and when the distance becomes less than 100 cm, the speed of the host vehicle decreases, and when the distance becomes less than 50 cm, the host vehicle stops. Then at the end, we move the lead vehicle which is controlled by Bluetooth and we see that the host vehicle moves forward again without starting when the distance exceeds 50 cm.

In the theoretical part, we assume that the initial distance is d_{rel}=110 cm and that the initial longitudinal speed of the lead vehicle is v_{x_h}=22.22 m/s.

The comparison is made with the results obtained in the reference document [37], knowing that we used the same parameters as those used by this document. The parameters of RBFNN are given in Table II.

TABLE II. RBFNN PARAMETERS FOR THE APPROXIMATION OF K(x, w)

Description	Parameter	Value
Structure of RBFNN	-	3-6-1
Centre point of the Gaussian function	c_{ij}	3×[-0.34 0.04 0.67 0.04 -1.67 -0.34; -0.34 0.04 0.67 0.04 -1.67 -0.34; -0.34 0.04 0.67 0.04 -1.67 -0.34]
Width value of Gaussian function	b_j	$[3\ 3\ 1\ 1\ 3\ 3]^T$
Adaptive parameter	γ	500

Fig. 11 shows that the longitudinal speed obtained by STSMC or NTSMC based on NN corresponded to the desired longitudinal speed in all cases, even in the transitory cases, with a low error. The maximum error during the use of the STSMC controller is equal to 0.00633, while the maximum error during the use of the NTSMC–based on NN controller is equal to 0.00632. Thus, both commands are effective. However, from Fig. 12, we see that our proposed controller NTSMC based on NN is slightly better than STSMC controller.

Our proposed controller NTSMC_NN allows us to obtain better results such that the maximum error is equal to 0.00632 m/s comparable to the results obtained by RBF_NTSMC [37] such that the maximum error is equal to 0.665 m/s, and also we note that the results obtained by HMPC [38] (when the road slope angle i_r = 0.3) are not satisfactory, so the maximum error is equal to 1.5 m/s. The longitudinal speed of the host vehicle used is not above 15 m/s. It's important to note that the parameters used in this system [38] are not the parameters we used in our system.

The errors obtained when using the STSMC control method or the second method when using the NTSMC-based on NN control are very low, as shown in Fig. 12. Do not exceed $2.4\ 10^{-3}$ in normal cases, and $6.4\ 10^{-3}$ in critical cases. And we see that the error curve of NTSMC based on NN control proposed is always lower than that of STSMC control.

Our results are considerable and the controller is very efficient and robust. We can see this performance in the illustrations, particularly Fig. 11 and Fig. 12.

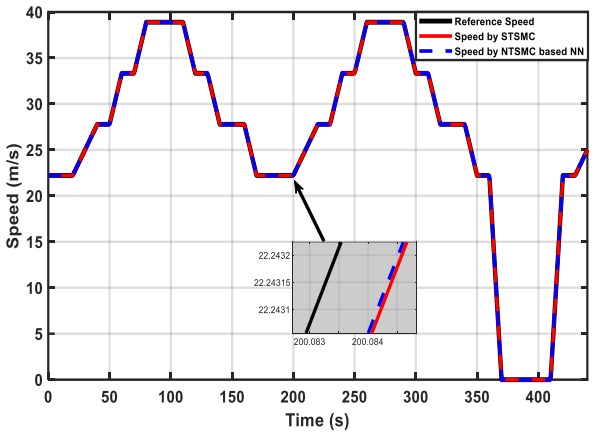

Fig. 11. Speed reference and controlled

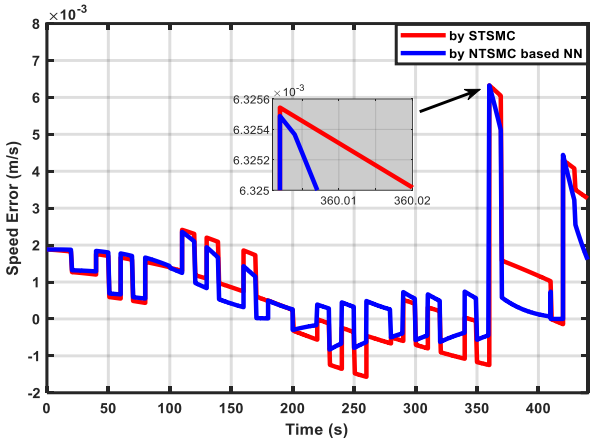

Fig. 12. Speed error

The traction controller curve in Fig. 13 allows the autonomous automobile to accelerate to follow the one in front, which follows the reference speed by its role. In normal cases the amplitude of this controller does not exceed 450 N but in critical cases, that is, when the automobile needs maximum speed to accelerate in order to follow the automobile that is moving located in front, the controller reaches an amplitude of 973.3 N.

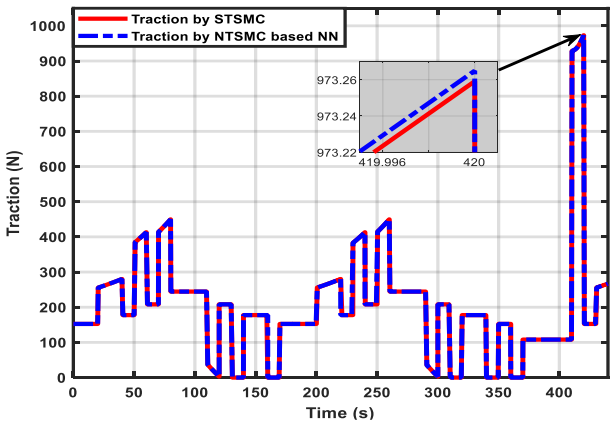

Fig. 13. Traction controller

When the distance between automobiles is reduced, we see from Fig. 14 that the brake controller enables the automobile to brake. In the normal case, that is, the distance is greater than 50 cm and less than 100 cm, the amplitude of the controller brake does not exceed 53 N, and to stop the

automobile in case the distance is less than 50 cm, the amplitude of this controller expects 712.9 N.

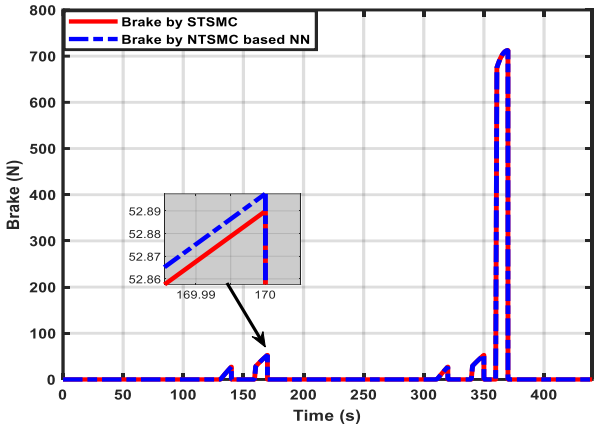

Fig. 14. Brake controller

V. CONCLUSION

The paper proposes the study of Adaptive Cruise Control (ACC) in a practical and theoretical ways, STSMC and NTSMC based on NN controllers have been introduced in this study. Neural networks are used to estimate the parameter of the reaching law term. According to the theoretical simulations, the STSMC and NTSMC based on NN have better results, such as the longitudinal speed obtained by our automobile control using STSMC or NTSMC-based on NN, is almost the same as the desired speed. The two controllers STSMC and NTSMC based on NN are efficient and robust with a small improvement of NTSMC-based on NN thanks to the integration of neural network. Our proposed NTSMC-based on NN controller offers better results compared to RBF_NTSMC controller and also HMPC. Our proposal to create an autonomous automobile prototype focused on the study of adaptive cruise control was made. The implementation of our ACC program in the Arduino board has been carried out. Our autonomous automobile prototype has successfully passed all the proposed tests.

In future research, we wish to implement our ACC program on a real automobile equipped with a microcontroller and sensors and actuators in order to test and develop this program. Implementing our program on a real automobile requires modifying the parameters of the test automobile in our program, which requires modifying the controller parameters in our program as well, and this is among the challenges that await us for the practical implementation.

REFERENCES

[1] B. L. Widjiantoro, M. Wafi, and K. Indriawati, "Non-Linear Estimation using the Weighted Average Consensus-Based Unscented Filtering for Various Vehicles Dynamics towards Autonomous Sensorless Design," *Journal of Robotics and Control (JRC)*, vol. 4, no. 1, pp. 95-107, 2023, doi: 10.18196/jrc.v4i1.16164.

[2] N. Abu, W. Bukhari, M. Adli, and A. Ma'arif, "Optimization of an Autonomous Mobile Robot Path Planning Based on Improved Genetic Algorithms," *Journal of Robotics and Control (JRC)*, vol. 4, no. 4, pp. 557-571, 2023, doi: 10.18196/jrc.v4i4.19306.

[3] N. Van, N. Tien, N. Luong, and H. Duyen, "Energy Consumption Minimization for Autonomous Mobile Robot: A Convex Approximation Approach," *Journal of Robotics and Control (JRC)*, vol. 4, no. 3, pp. 403-412, 2023, doi: 10.18196/jrc.v4i3.17509.

[4] F. Umam, M. Fuad, I. Suwarno, A. Ma'arif, and W. Caesarendra, "Obstacle Avoidance Based on Stereo Vision Navigation System for Omni-directional Robot," *Journal of Robotics and Control (JRC)*, vol. 4, no. 2, pp. 227-242, 2023, doi: 10.18196/jrc.v4i2.17977.

[5] L. Hanh and V. Cong, "Path Following and Avoiding Obstacle for Mobile Robot Under Dynamic Environments Using Reinforcement Learning," *Journal of Robotics and Control (JRC)*, vol. 4, no. 2, pp. 157-164, 2023, doi: 10.18196/jrc.v4i2.17368.

[6] A. Reddy, V. Chembuly, and V. Rao, "Modelling and Simulation of a Redundant Agricultural Manipulator with Virtual Prototyping," *Journal of Robotics and Control (JRC)*, vol. 4, no. 1, pp. 83-94, 2023, doi: 10.18196/jrc.v4i1.17121.

[7] M. V. Sreenivas Rao and M. Shivakumar, "IR Based Auto-Recharging System for Autonomous Mobile Robot," *Journal of Robotics and Control (JRC)*, vol 2, no 4, pp. 244–251, 2021, doi: doi: 10.18196/jrc.2486.

[8] Z. Abdullah, S. Shneen, and H. Dakheel, "Simulation Model of PID Controller for DC Servo Motor at Variable and Constant Speed by Using MATLAB," *Journal of Robotics and Control (JRC)*, vol. 4, no. 1, pp. 54-59, 2023, doi: 10.18196/jrc.v4i1.15866.

[9] A. Carullo and M. Parvis, "An ultrasonic sensor for distance measurement in automotive applications," in *IEEE Sensors Journal*, vol. 1, no. 2, pp. 143, 2001, doi: 10.1109/JSEN.2001.936931.

[10] N. El Youssfi, R. El Bachtiri, R. Chaibi, and E. H. Tissir, "Static output-feedback H ∞ control for T–S fuzzy vehicle lateral dynamics," in *SN Applied Sciences*, p. 101, 2020, doi: 10.1007/s42452-019-1897-y.

[11] N. El Fezazi, E. H. Tissir, F. El Haoussi, F. A. Bender, and A. R. Husain, "Controller Synthesis for Steer-by-Wire System Performance in Vehicle," *Iran J. Sci. Technol. Trans. Electr. Eng.*, vol. 43, no 4, p. 813-825, 2019, doi: 10.1007/s40998-019-00204-8.

[12] J. Mrazgua, E. H. Tissir, and M. Ouahi, "Frequency domain H ∞ control design for active suspension systems," *DCDS-S*, vol. 15, no 1, p. 197-212, 2021, doi: 10.3934/dcdss.2021036.

[13] M. Loubna, E. H. Tissir, and O. Mohamed, "H ∞ Control For Vehicle Active Suspension Systems In Finite Frequency Domain," *2019 5th International Conference on Optimization and Applications (ICOA)*, p. 1-5, 2019, doi: 10.1109/ICOA.2019.8727652.

[14] Y. Jiang, L. Cai, and X. Jin, "Optimization of Adaptive Cruise Control system Controller: using Linear Quadratic Gaussian based on Genetic Algorithm, Electrical Engineering and Systems Science - Systems and Control," *arXiv.1911.08349*, 2020.

[15] J. Pauwelussen and P. J. Feenstra, "Driver behavior analysis during ACC activation and deactivation in a real traffic environment," *IEEE Trans. Intell. Transp. Syst.*, vol. 11, no. 2, pp.329–338, 2010.

[16] Y. Irawan, M. Muhardi, R. Ordila, and R. Diandra, "Automatic Floor Cleaning Robot Using Arduino and Ultrasonic Sensor," *Journal of Robotics and Control (JRC)*, vol 2, no 4, 2021, doi: 10.18196/jrc.2485.

[17] P. Chotikunnan and R. Chotikunnan, "Dual Design PID Controller for Robotic Manipulator Application," *Journal of Robotics and Control (JRC)*, vol. 4, no. 1, pp. 23-34, 2023, doi: 10.18196/jrc.v4i1.16990.

[18] E. Nugroho, J. Setiawan, and M. Munadi, "Handling Four DOF Robot to Move Objects Based on Color and Weight using Fuzzy Logic Control," *Journal of Robotics and Control (JRC)*, vol. 4, no. 6, pp. 769-779, 2023, doi: 10.18196/jrc.v4i6.20087.

[19] J. Díaz-Téllez, R. García-Ramírez, J. Pérez-Pérez, J. Estevez-Carreón, and M. Carreón-Rosales, "ROS-based Controller for a Two-Wheeled Self-Balancing Robot," *Journal of Robotics and Control (JRC)*, vol. 4, no. 4, pp. 491-499, 2023, doi: 10.18196/jrc.v4i4.18208.

[20] F. A. Candelas *et al*., "Experiences on using Arduino for laboratory experiments of Automatic Control and Robotics," *IFAC-PapersOnLine*, vol. 48, no. 29, pp. 105-110, 2015, doi: 10.1016/j.ifacol.2015.11.221.

[21] A. Araújo, D. Portugal, M. S. Couceiro, and R. P. Rocha, "Integrating Arduino-based educational mobile robots in ROS," *Journal of Intelligent & Robotic Systems*, vol. 77, no. 2, pp. 281-298, 2015.

[22] R. Alika, E. M. Mellouli, and E. H. TISSIR, "Adaptive modified super-twisting sliding mode control based on PSO with neural

network for lateral dynamics of autonomous vehicle," *International Journal of Modelling, Identification and Control*, vol. 42, no. 4, 2023, doi: 10.1504/IJMIC.2023.131207.

[23] E. M. Mellouli, R. Naoual, and I. Boumhidi, "A new modified sliding mode controller based fuzzy logic for a variable speed wind turbine," *International Journal of Ecology & Development*, vol. 32, pp. 44–53, 2017.

[24] E. M. Mellouli, C. Zakaria, A. Mohammed, and I. Boumhidi, "A New Robust Adaptive Fuzzy Sliding Mode Controller for a Variable Speed Wind Turbine," *International Review of Automatic Control (IREACO)*, vol. 8, p. 338, 2015, doi: 10.15866/ireaco.v8i5.7192.

[25] M. Huynh, H. Duong, and V. Nguyen, "A Passivity-based Control Combined with Sliding Mode Control for a DC-DC Boost Power Converter," *Journal of Robotics and Control (JRC)*, vol. 4, no. 6, pp. 780-790, 2023, doi: 10.18196/jrc.v4i6.20071.

[26] E. M. Mellouli, S. Sefriti and I. Boumhidi, "Combined fuzzy logic and sliding mode approach's for modelling and control of the two link robot," *2012 IEEE International Conference on Complex Systems (ICCS)*, pp. 1-6, 2012, doi: 10.1109/ICoCS.2012.6458599.

[27] P. Chotikunnan, R. Chotikunnan, A. Nirapai, A. Wongkamhang, P. Imura, and M. Sangworasil, "Optimizing Membership Function Tuning for Fuzzy Control of Robotic Manipulators Using PID-Driven Data Techniques," *Journal of Robotics and Control (JRC)*, vol. 4, no. 2, pp. 128-140, 2023, doi: 10.18196/jrc.v4i2.18108.

[28] M. Auzan, D. Lelono, and A. Dharmawan, "Humanoid Walking Control Using LQR and ANFIS," *Journal of Robotics and Control (JRC)*, vol. 4, no. 4, pp. 548-556, 2023, doi: 10.18196/jrc.v4i4.16444.

[29] M. Zadehbagheri, A. Ma'arif, R. Ildarabadi, M. Ansarifard, and I. Suwarno, "Design of Multivariate PID Controller for Power Networks Using GEA and PSO," *Journal of Robotics and Control (JRC)*, vol. 4, no. 1, pp. 108-117, 2023, doi: 10.18196/jrc.v4i1.15682.

[30] H. Tran and T. Dang, "An Ultra Fast Semantic Segmentation Model for AMR's Path Planning," *Journal of Robotics and Control (JRC)*, vol. 4, no. 3, pp. 424-430, 2023, doi: 10.18196/jrc.v4i3.18758.

[31] K. Dahmane *et al*., "Hybrid MPPT Control: P&O and Neural Network for Wind Energy Conversion System," *Journal of Robotics and Control (JRC)*, vol. 4, no. 1, pp. 1-11, 2023, doi: 10.18196/jrc.v4i1.16770.

[32] M. Karis, H. Kasdirin, N. Abas, W. Saad, M. Zainudin, N. Ali, and M. Aras, "Analysis of ANN and Fuzzy Logic Dynamic Modelling to Control the Wrist Exoskeleton," *Journal of Robotics and Control (JRC)*, vol. 4, no. 4, pp. 572-583, 2023, doi: 10.18196/jrc.v4i4.19299.

[33] M. Shamseldin, "Real-Time Inverse Dynamic Deep Neural Network Tracking Control for Delta Robot Based on a COVID-19 Optimization," *Journal of Robotics and Control (JRC)*, vol. 4, no. 5, pp. 643-649, 2023, doi: 10.18196/jrc.v4i5.18865.

[34] R. Alika, E. M. Mellouli, and E. H. TISSIR, "Adaptive Higher-Order Sliding Mode Control Based Fuzzy Logic T-S for Lateral Dynamics of Autonomous Vehicles," In *2021 12th International Conference on Information and Communication Systems (ICICS)*, p. 358-363, 2021, doi: 10.1109/ICICS52457.2021.9464623.

[35] R. Alika, E. M. Mellouli, and E. H. TISSIR, "Optimization of Higher-Order Sliding Mode Control Parameter using Particle Swarm Optimization for Lateral Dynamics of Autonomous Vehicles," In *2020 1st International Conference on Innovative Research in Applied Science, Engineering and Technology (IRASET)*, p. 1-6, 2020, doi: 10.1109/IRASET48871.2020.9092119.

[36] R. Alika, E. M. Mellouli, and E. H. Tissir, "Disturbance Observer-Based Adaptive Sliding Mode Control for Autonomous Vehicles," In: *Artificial Intelligence and Smart Environment. ICAISE 2022*, vol 635, pp. 359–366, 2022, doi: 10.1007/978-3-031-26254-8_51.

[37] S. Wang, Y. Hui, X. Sun, and D. Shi, "Neural Network Sliding Mode Control of Intelligent Vehicle Longitudinal Dynamics," *IEEE Access*, vol. 7, p. 162333-162342, 2019, doi: 10.1109/ACCESS.2019.2949992

[38] X. Sun, Y. Cai, S. Wang, X. Xu, and L. Chen, ''Optimal control of intelligent vehicle longitudinal dynamics via hybrid model predictive control,'' *Robot. Auton. Syst.*, vol. 112, pp. 190–200, 2019, doi: 10.1016/j.robot.2018.11.020.

[39] H. Wang, Z. Zuo, Y. Wang, H. Yang, and C. Hu, "Longitudinal Velocity Regulation of UGVs: A Composite Control Approach for Acceleration and Deceleration," in *IEEE Transactions on Intelligent Transportation Systems*, vol. 24, no. 10, pp. 11096-11106, 2023, doi: 10.1109/TITS.2023.3274106.

[40] C. Zhang, X. Wei, Z. Wang, H. Zhang, and X. Guo, "T-S fuzzy-model-based adaptive cruise control for longitudinal car-following considering vehicle lateral stability," *Intell Robot*, vol. 2, no. 4, pp. 371-90, 2022, doi: 10.20517/ir.2022.26.

[41] J. Susilo, A. Febriani, U. Rahmalisa, and Y. Irawan, "Car Parking Distance Controller Using Ultrasonic Sensors Based On Arduino Uno" *Journal of Robotics and Control (JRC)*, vol 2, no 5, 2021, doi: 10.18196/jrc.25106.

[42] R. H. Madhan and K. Priya, "Fully Automated Cruise Control System Using Ultrasonic Sensor," *Biomed. Pharmacol. J.*, vol. 8, no. 1, 2015, doi: 10.13005/bpj/612.

[43] N. C. Basjaruddin, K. Kuspriyanto, D. Saefudin, and I. Khrisna Nugraha, "Developing Adaptive Cruise Control Based on Fuzzy Logic Using Hardware Simulation", *International Journal of Electrical and Computer Engineering (IJECE)*, vol. 4, no. 6, pp. 944-951, 2014, doi: 10.11591/ijece.v4i6.6734.

[44] L. Nouvelière and S. Mammar, "Experimental vehicle longitudinal control using a second order sliding mode technique," *Control Engineering Practice*, vol. 15, no 8, p. 943-954, 2007, doi: 10.1016/j.conengprac.2006.11.011.

[45] R. Rajamani. *Vehicle Dynamics and Control*. Springer Science & Business Media, 2012. doi: 10.1007/978-1-4614-1433-9.

[46] X. Ji, X. He, C. Lv, and Y. Liu, "Adaptive-neural-network-based robust lateral motion control for autonomous vehicle at driving limits", In *Control Engineering Practice*, vol. 76, 2018, doi: 10.1016/j. conengprac.2018.04.007.

[47] K. Rani and N. Kumar, "An optimal control approach for hybrid motion/force control of coordinated multiple nonholonomic mobile manipulators using neural network", *International Journal of Modelling*, vol. 37, no. 2, pp.164–175, 2021, doi: 10.1504/IJMIC. 2021.120207.

[48] E. M. Mellouli, S. Massou, and I. Boumhidi, "Optimal Robust Adaptive Fuzzy Tracking Control without Reaching Phase for Nonlinear System", *Journal of Control Science and Engineering*, vol. 2013, no 498461, p. 7, 2013, doi: 10.1155/2013/498461.

[49] T. I. Nasution and P. F. A. Azis, "MPU-6050 Wheeled Robot Controlled Hand Gesture Using L298N Driver Based on Arduino," In *Journal of Physics: Conference Series*, vol. 2421, no. 1, p. 012022, 2023.

[50] M. M. Gabriel and K. P. Kuria, "Arduino Uno, Ultrasonic Sensor HC-SR04 Motion Detector with Display of Distance in the LCD," *International Journal of Engineering Research & Technology (IJERT)*, vol. 09, no. 05, 2020, doi: 10.17577/IJERTV9IS050677.

[51] Supriyono and Marjuki, "Ultrasonic Sensor Parking Assistant With Arduino Uno," *International Journal of Advanced Research in Engineering and Technology (IJARET)*, vol. 11, no. 5, pp. 26-33, , 2020, doi: 10.34218/IJARET.11.5.2020.004.

[52] A. Buachoom, A. Thedsakhulwong, and S. Wuttiprom, "An Arduino board with ultrasonic sensor investigation of simple harmonic motion," in *Journal of Physics: Conference Series*, vol. 1380, no. 1, p. 012098, 2019, doi: 10.1088/1742-6596/1380/1/012098.

[53] H. Marhoon, A. Alanssari, and N. Basil, "Design and Implementation of an Intelligent Safety and Security System for Vehicles Based on GSM Communication and IoT Network for Real-Time Tracking," *Journal of Robotics and Control (JRC)*, vol. 4, no. 5, pp. 708-718, 2023, doi: 10.18196/jrc.v4i5.19652.

[54] L. Louis, "working principle of Arduino and u sing it," *International Journal of Control, Automation, Communication and Systems (IJCACS)*, vol. 1, no. 2, pp. 21-29, 2016, doi: 10.22214/ijraset.2022.41784.

[55] G. Organtini, "Arduino as a tool for physics experiments," in *Journal of Physics: Conference Series*, vol. 1076, no. 1, p. 012026, 2018, doi: 10.1088/1742-6596/1076/1/012026.

[56] R. Stiawan, A. Kusumadjati, N. S. Aminah, M. Djamal, and S. Viridi, "An Ultrasonic Sensor System for Vehicle Detection Application," *Journal of Physics: Conference Series*, vol. 1204, no. 1, p. 012017, 2019, doi: 10.1088/1742-6596/1204/1/012017.

[57] S. Monisha, R. Ratan, and S. K. Luthra, "Design & Development of Smart Ultrasonic Distance Measuring Device," *International Journal*

of Innovative Research in Electronics and Communications (IJIREC), vol. 2, no. 3, pp. 19-23, 2015.

[58] N. Soni, S. Maheshwari, B. K. Sahu, B. Jain, and G. Shrivastava, "Distance Measurement Using Ultrasonic Sensor and Arduino," *International Journal of Engineering Science and Computing*, vol. 7, no. 3, pp. 1-2, 2017.

[59] A. Ubaidillah and H. Sukri, "Application of Odometry and Dijkstra Algorithm as Navigation and Shortest Path Determination System of Warehouse Mobile Robot," *Journal of Robotics and Control (JRC)*, vol. 4, no. 3, pp. 413-423, 2023, doi: 10.18196/jrc.v4i3.18489.

[60] L. H. Goon, A. N. I. M. Isa, C. H. Choong, and W. A. F. W. Othman, "Development of Simple Automatic Floor Polisher Robot using Arduino," *International Journal of Engineering Creativity & Innovation*, vol. 1, no. 1, pp. 17-23, 2019.

[61] A. Ma'arif and N. R. Setiawan, "Control of DC Motor Using Integral State Feedback and Comparison with PID: Simulation and Arduino Implementation," *Journal of Robotics and Control (JRC)*, vol. 2, no. 5, pp. 456-461, 2021, doi: 10.18196/jrc.25122.